Computational prediction of two-dimensional group-IV mono-chalcogenides

Arunima K. Singh and Richard G. Hennig

Citation: Appl. Phys. Lett. **105**, 042103 (2014); doi: 10.1063/1.4891230
View online: http://dx.doi.org/10.1063/1.4891230
View Table of Contents: http://aip.scitation.org/toc/apl/105/4
Published by the American Institute of Physics

Computational prediction of two-dimensional group-IV mono-chalcogenides

Arunima K. Singh and Richard G. Hennig[a)]
Department of Materials Science and Engineering, Cornell University, Ithaca, New York 14853, USA

(Received 2 June 2014; accepted 14 July 2014; published online 28 July 2014)

Density functional calculations determine the structure, stability, and electronic properties of two-dimensional materials in the family of group-IV monochalcogenides, MX (M = Ge, Sn, Pb; X = O, S, Se, Te). Calculations with a van der Waals functional show that the two-dimensional IV-VI compounds are most stable in either a highly distorted NaCl-type structure or a single-layer litharge type tetragonal structure. Their formation energies are comparable to single-layer MoS_2, indicating the ease of mechanical exfoliation from their layered bulk structures. The phonon spectra confirm their dynamical stability. Using the hybrid HSE06 functional, we find that these materials are semiconductors with bandgaps that are generally larger than for their bulk counterparts due to quantum confinement. The band edge alignments of monolayer group IV-VI materials reveal several type-I and type-II heterostructures, suited for optoelectronics and solar energy conversion.
 [http://dx.doi.org/10.1063/1.4891230]

The synthesis of graphene, a two-dimensional (2D) phase of carbon, has paved the way for the discovery and synthesis of many other 2D materials.[1–9] Recent theoretical and experimental studies have investigated the possibility of realizing many more 2D materials, such as GaN,[5,10] MoS_2,[11] CrS_2,[12] BN,[13] GaSe, and InSe.[7,14]

Single-layer materials present the ultimate scaling in thickness and exhibit electronic, optical, and mechanical properties different from their bulk counterparts. For instance, recent experimental studies have shown that single-layer MoS_2 exhibits a wider bandgap than its three-dimensional (3D) bulk counterpart.[2,15] Likewise, pristine graphene differs from graphite withstanding strains exceeding 20%,[16,17] as opposed to an elastic strain of up to 0.1% for graphite.[18] With the uniqueness of the 2D materials' structures and properties, it is expected that some of these materials will exhibit unforeseen properties that present invaluable opportunities for innovative applications. This motivates the ongoing search for 2D materials with unusual properties.[19]

To identify 2D materials with unusual properties for nano-electronics or energy conversion, it is advantageous to start from bulk phases that have proven useful for such applications. Bulk group-IV mono-chalcogenides have extensively been studied due to their potential for applications in the fields of catalysis, opto-electronics, and lithium ion batteries.[20] For example, photovoltaic cells based on SnS are superior than their Cd and Pb based alternatives because of non-toxicity and high efficiency exceeding 15%.[21] In contrast to their bulk counterparts, only a few studies explored the single-layer group-IV mono-chalcogenides. Recently, Tritsaris *et al.*[21] studied the opto-electronic properties of SnS as a function of number of layers in its distorted NaCl-type structure. Li *et al.*[22] and Ma *et al.*[23] have synthesized multi-layer nanosheets of SnSe. A comprehensive study of the stability and properties of group IV-VI single-layered materials is still missing.

In this Letter, we use density-functional theory (DFT) to systematically characterize previously unknown single-layer group-IV monochalcogenides (MX). We identify the lowest-energy 2D structure among five candidate structures that are shown in Fig. 1. The thermodynamic stability is given by the formation energy of each 2D MX relative to the corresponding bulk compound, and the dynamical stability is determined by the phonon spectrum. We find the 2D MX (X = S, Se, Te) are stable in the distorted-NaCl (d-NaCl) structure. 2D SnO and PbO are stable in the tetragonal litharge structure. Hybrid-functional calculations characterize how the reduced dimensionality alters the electronic structures of the MX. We construct a multi-dimensional diagram to illustrate the relationship between lattice parameters, effective masses, and bandgaps of these 2D materials to supplement materials selection for electronic device design, analogous to 3D materials selection diagrams. To further assist device design, we

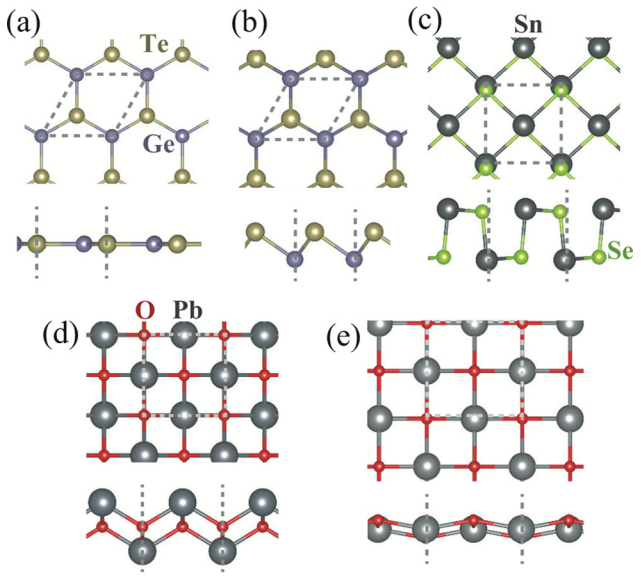

FIG. 1. Top and side view of the (a) planar hexagonal, (b) buckled hexagonal, (c) distorted-NaCl, (d) litharge, and (e) inverted litharge structures.

[a)]Electronic mail: rhennig@cornell.edu.

determine the 2D materials' band edge positions and identify several types I and II heterostructures.

All calculations are based on DFT using the projector augmented wave method as implemented in the plane-wave code VASP.[24–26] For the structural relaxations and energy calculations, we employ the optB88-vdW functional, which includes van der Waals (vdW) interactions.[27,28] We optimize all structures until forces and in-plane stresses are below 1 meV/Å and 0.01 GPa, respectively. The phonon calculations are performed with the PBE functional. To overcome the problem of bandgap underestimation in semilocal exchange-correlation functionals, we use the HSE06 hybrid functional for calculating the band structures.[29,30] A cutoff energy of 520 eV for the plane wave basis set ensures an accuracy of the energy of 1 meV/atom. The k-point sampling employs for the 2D materials at least an $18 \times 18 \times 3$ mesh for the vdW functional, a $12 \times 12 \times 1$ mesh for the more expensive HSE06 functional, and a $20 \times 20 \times 20$ mesh for the bulk systems resulting in a similar accuracy as the cutoff-energy convergence. For the 2D materials, a vacuum spacing of 18 Å ensures that the interactions between the layers are negligible. More expensive, HSE06 calculations are performed with a 10 Å vacuum spacing.

The energetic stability of the proposed 2D MX with respect to their bulk forms is determined by the energy difference between the 2D and bulk compounds, $\Delta E = E_{2D}/N_{2D} - E_{bulk}/N_{bulk}$. The bulk MX compounds PbX (X = S, Se, Te) and SnTe occur in the NaCl structure. The bulk MX (M = Ge, Sn and X = S, Se) adopt a distorted rock salt (d-NaCl) structure with orthorhombic space group *Pnma*, where double layers of metal mono-chalcogenide atoms are separated by a van der Waals gap. Bulk SnO and PbO occur in the litharge structure with tetragonal space group *P*4/*nmm* that consists of buckled layers in which O is tetrahedrally bonded to the metal atoms. Bulk GeTe crystallizes in a layered rhombohedral structure with space group *R*3*m* that consists of buckled hexagonal layers.[31] In contrast to the other MX, GeO is unstable at ambient conditions. Thus, for the formation energy of 2D GeO we assume a reaction of Ge and GeO_2. Ge crystallizes in the diamond structure and GeO_2 in a hexagonal structure with space group $P3_121$.

Fig. 1 illustrates the five different 2D structures considered for the single-layer MX. They are chosen because they either correspond to individual layers of the layered bulk MX phases, e.g., the buckled hexagonal, litharge, or d-NaCl structures, or are commonly observed in other 2D materials, e.g., the planar hexagonal structure.[5,6,32] 2D materials with vdW-bonded layered bulk counterparts exhibit structures similar to individual bulk layers, e.g., graphene, metal dichalcogenides, group-III monochalcogenides,[1,4,7,11,14] and 2D hexagonal structure are common for several materials with non-layered bulk structures, e.g., ZnO and GaN.[3,5]

Fig. 2 shows the formation energy, ΔE, of the lowest energy 2D MX structure. Single-layer PbO and SnO, consistent with their bulk structure, are most stable in the litharge structure with space group *P*4/*nmm*, which is illustrated in Fig. 1(d). All other MX compounds prefer the d-NaCl type structure with space group $Pmn2_1$ illustrated in Fig. 1(c), which is consistent with the bulk NaCl or d-NaCl structures of these materials. Even 2D GeTe has a lower energy in the

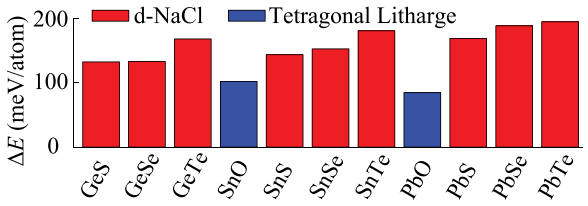

FIG. 2. Formation energies of the lowest energy single-layer MX structures relative to the corresponding bulk compounds. Not shown in the figure, the formation energy of GeO in the d-NaCl structure is 615 meV/atom.

d-NaCl structure although the bulk structure consists of stacks of buckled hexagonal layers. For most of the 2D materials that are stable in the d-NaCl structure, the group-IV atoms are in the top and bottom most position and $a \neq b$. The exceptions are 2D PbSe and PbTe, which relax such that $a = b$, and 2D SnTe and PbTe, which have the chalcogen atoms in the top and bottom most position.

In the GeX (X = S, Se, Te) compounds the formation energies of the buckled hexagonal, litharge, and inverted litharge structures are all within 70 meV/atom of the energy of the most stable d-NaCl structure. The SnX and PbX 2D compounds are increasingly more selective for the d-NaCl structure and the trend of the structure selectivity Pb > Sn > Ge can be a useful guide for synthesis efforts. The supplementary material shows the formation energies of the 2D MX for all five structures and the structural parameters of the lowest-energy structures.[33]

The formation energies of the lowest energy 2D MX structures range from 80 to 200 meV/atom with the exception of GeO, which has a high formation energy of 0.6 eV/atom. With such low formation energies, it is expected that common synthesis techniques of 2D materials such as chemical-vapor deposition (CVD) or molecular-beam epitaxy (MBE) can be used to grow these materials. Since the GeX (X = S, Se, Te) compounds have comparable energies in the buckled hexagonal, litharge, inverted litharge, and d-NaCl structures it may be possible to grow any of these structure by selection of a suitable substrate that is symmetry and lattice-matched with these 2D structures. In addition to CVD and MBE, exfoliation techniques are viable for the synthesis of the single-layer MX that have layered 3D parent structures, such as SnO, PbO, and the MX (M = Ge, Sn and X = S, Se). For GeTe, exfoliation may result in the buckled hexagonal structure instead of the 70 meV/atom lower d-NaCl one as this is the structure of the layers in the bulk. Furthermore, the range of formation energies is consistent with weak electrostatic and vdW interactions and is comparable or only slightly larger than formation energies of experimentally synthesized BN, graphene, and MoS_2.[9,34] In contrast, the large formation energy of GeO of 0.6 eV/atom is more similar to that of silicene and limits the possibility of its synthesis by typical 2D material synthesis techniques unless a suitable stabilizing substrate can be found.[35]

To investigate the dynamical stability of the predicted single-layer materials, we calculate their phonon spectra, using density-functional perturbation theory.[36,37] A dynamic instability in the structure is reflected in an imaginary phonon branch for some k-points in the Brillouin zone. We find that all the MX are dynamically stable (see supplementary material[33] for the phonon spectra).

Fig. 3 shows the site projected band structures obtained using the HSE06 hybrid functional. We observe that the valence band maxima (VBM) are dominated by the *p* orbitals of the chalcogen atoms that are hybridized with *s* and *p* orbitals of the group-IV atoms. The conduction band minima (CBM), on the other hand, are dominated by the empty *s* orbitals of the group-IV atoms. Comparison with experimental bandgaps of the bulk materials (see supplementary material[33]) shows that the reduction in dimensionality for the 2D materials changes the bandgap type for several materials and generally increases the gap, which is due to the quantum confinement in the 2D materials that is caused by the removal of the interaction of the *p*-orbitals across the interlayer region. Among the 2D IV-VI materials, GeS, GeSe, and PbO are direct bandgap semiconductors while all others exhibit an indirect gap. For each group-IV family, the bandgap increases with decreasing size of the chalcogen atoms. The stronger *s*–*p* hybridization for the smaller chalcogen atoms and corresponding group-IV materials increases the splitting between bonding and antibonding states and hence opens up the bandgap.[38]

Fig. 4 shows the bandgaps, electron and hole effective masses for the 2D IV-VI compounds as a function of the lattice parameters *a* and *b*. Most of the bandgaps lie within the range of visible light, indicating that these 2D materials may be useful for optoelectronic or solar energy conversion applications. The electron and hole effective masses are determined by the second derivative of the HSE06 band structures at the CBM and VBM, respectively (values given in the supplementary material[33]). The effective masses affect carrier mobilities of the 2D materials. We find that the effective masses for most group IV-VI materials are comparable

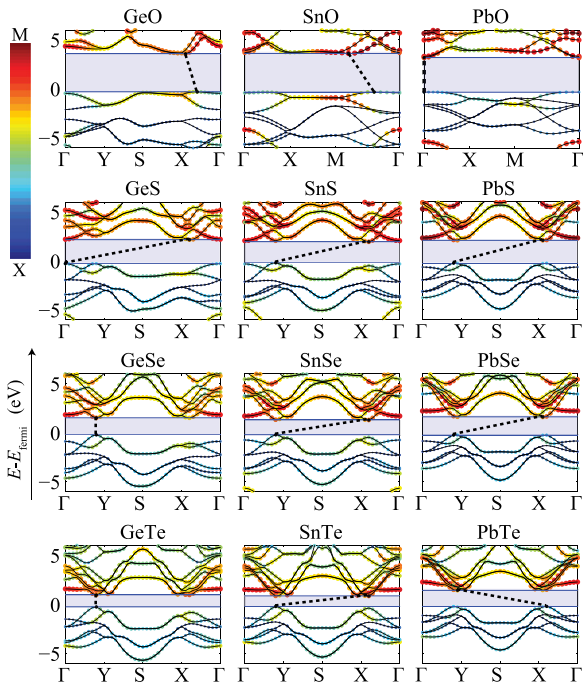

FIG. 3. Electronic band structure of the group IV-VI materials projected onto the M and X atoms for the most stable structures. The symbol sizes and colors denote the weights of the M and X sites. The shaded blue region indicates the bandgap, and the dashed lines indicate the bandgap type. The VBM is set to zero.

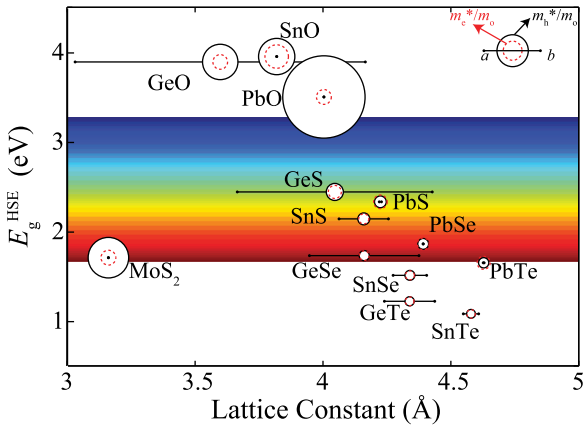

FIG. 4. HSE06 band gaps, effective masses, and lattice constants of the 2D IV-VI materials. The inner and outer radii represent the electron and hole effective mass, respectively. The ends of the horizontal lines indicate the *a* and *b* lattice parameters. A sketch of the visible spectrum is overlaid to aid visualization of the bandgap size.

to common semiconductors such as silicon and single-layer MoS_2.[39,40] We also find an unusually large hole effective mass for 2D PbO, which was already reported in a previous study.[41]

For the design of devices, it is important to know the intrinsic band offsets between the various 2D materials. Fig. 5 shows the band edge alignment of the 2D IV-VI compounds obtained using the HSE06 functional. We observe that the CBM and VBM energies of the MX compounds increase for larger atomic numbers of M, while for larger atomic numbers of the X, the VBM energy increases but the CBM energy decreases. The only exceptions are the VBM of PbSe, which is 0.06 eV lower than VBM of SnSe, and the VBM of PbTe, which is 0.25 eV lower than GeTe and 0.5 eV lower than SnTe. Comparing the band edge positions of the 2D MX with the redox potentials of water shows that, in contrast to the group-III monochalcogenides[7] and transition-metal dichalcogenides,[34] the group-IV monochalcogenides require a bias potential to be suitable for photocatalytic water splitting.[42]

To create heterostructures of the 2D MX, a small lattice mismatch is desirable. The mismatch between the GeTe-SnSe/SnTe/PbSe/PbTe, SnO-PbO, SnS-PbS, SnSe-PbS/PbSe, and SnTe-PbTe materials is less than 5% enabling heterostructures without structural defects. We find that the band alignment for SnO-PbO and SnS-PbS is type II and for GeTe-SnSe/SnTe/PbSe/PbTe, SnSe-PbS/PbSe, and SnTe-PbTe is type I. In the type-II heterostructures, free electrons and holes will spontaneously separate into the different layers, which is useful for optoelectronics and solar energy conversion.

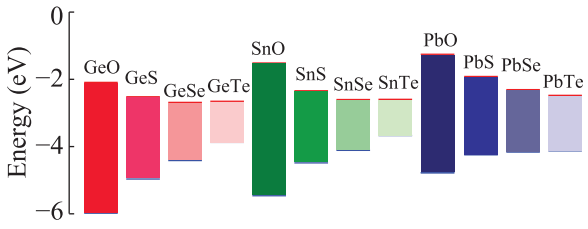

FIG. 5. Band alignment of the 2D IV-VI materials relative to the vacuum level for the HSE06 functional.

In summary, we have shown that the single-layer IV-VI compounds are stable in a distorted NaCl or litharge structure with formation energies comparable to single-layer MoS_2, indicating the ease of mechanical exfoliation from their layered bulk compounds. The phonon spectra confirm their dynamical stability. Using the HSE06 hybrid functional, we find that these materials are semiconductors with bandgaps that are generally larger than for their bulk counterparts due to the reduction in dimensionality. The band edge alignments of these single-layer materials reveal several types-I and II heterostructures, suited for optoelectronics and solar energy conversion.

This work was supported by the NSF through the Cornell Center for Materials Research under Award No. DMR-1120296 and in part by the CAREER Award No. DMR-1056587. This research used computational resources of the Texas Advanced Computing Center under Contract No. TG-DMR050028N.

[1]K. S. Novoselov, V. Falko, L. Colombo, P. R. Gellert, M. G. Schwab, and K. Kim, Nature **490**, 192 (2012).
[2]K. F. Mak, C. Lee, J. Hone, J. Shan, and T. F. Heinz, Phys. Rev. Lett. **105**, 136805 (2010).
[3]C. Tusche, H. L. Meyerheim, and J. Kirschner, Phys. Rev. Lett. **99**, 026102 (2007).
[4]C. Jin, F. Lin, K. Suenaga, and S. Iijima, Phys. Rev. Lett. **102**, 195505 (2009).
[5]H. L. Zhuang, A. K. Singh, and R. G. Hennig, Phys. Rev. B **87**, 165415 (2013).
[6]H. L. Zhuang and R. G. Hennig, Appl. Phys. Lett. **101**, 153109 (2012).
[7]H. L. Zhuang and R. G. Hennig, Chem. Mater. **25**, 3232 (2013).
[8]S. Lebègue, T. Björkman, M. Klintenberg, R. M. Nieminen, and O. Eriksson, Phys. Rev. X **3**, 031002 (2013).
[9]A. K. Singh, H. L. Zhuang, and R. G. Hennig, Phys. Rev. B **89**, 245431 (2014).
[10]C. L. Freeman, F. Claeyssens, N. L. Allan, and J. H. Harding, Phys. Rev. Lett. **96**, 066102 (2006).
[11]Q. H. Wang, K. Kalantar-Zadeh, A. Kis, J. N. Coleman, and M. S. Strano, Nat. Nanotechnol. **7**, 699 (2012).
[12]H. L. Zhuang, M. D. Johannes, M. N. Blonsky, and R. G. Hennig, Appl. Phys. Lett. **104**, 022116 (2014).
[13]D. Golberg, Y. Bando, Y. Huang, T. Terao, M. Mitome, C. Tang, and C. Zhi, ACS Nano **4**, 2979 (2010).
[14]D. J. Late, B. Liu, J. Luo, A. Yan, H. Matte, M. Grayson, C. Rao, and V. P. Dravid, Adv. Mater. **24**, 3549 (2012).
[15]A. Splendiani, L. Sun, Y. Zhang, T. Li, J. Kim, C.-Y. Chim, G. Galli, and F. Wang, Nano Lett. **10**, 1271 (2010).
[16]C. Lee, X. Wei, J. W. Kysar, and J. Hone, Science **321**, 385 (2008).
[17]F. Liu, P. Ming, and J. Li, Phys. Rev. B **76**, 064120 (2007).
[18]J. Feng, X. Qian, C.-W. Huang, and J. Li, Nat. Photonics **6**, 866 (2012).
[19]H. L. Zhuang and R. G. Hennig, JOM **66**, 366 (2014).
[20]P. D. Antunez, J. J. Buckley, and R. L. Brutchey, Nanoscale **3**, 2399 (2011).
[21]G. A. Tritsaris, B. D. Malone, and E. Kaxiras, J. Appl. Phys. **113**, 233507 (2013).
[22]L. Li, Z. Chen, Y. Hu, X. Wang, T. Zhang, W. Chen, and Q. Wang, J. Am. Chem. Soc. **135**, 1213 (2013).
[23]X.-H. Ma, K.-H. Cho, and Y.-M. Sung, CrystEngComm **16**, 5080 (2014).
[24]G. Kresse and J. Furthmüller, Phys. Rev. B **54**, 11169 (1996).
[25]P. E. Blöchl, Phys. Rev. B **50**, 17953 (1994).
[26]G. Kresse and D. Joubert, Phys. Rev. B **59**, 1758 (1999).
[27]J. P. Perdew, K. Burke, and M. Ernzerhof, Phys. Rev. Lett. **77**, 3865 (1996).
[28]J. Klimeš, D. R. Bowler, and A. Michaelides, Phys. Rev. B **83**, 195131 (2011).
[29]J. Heyd, G. E. Scuseria, and M. Ernzerhof, J. Chem. Phys. **118**, 8207 (2003).
[30]J. Heyd, J. E. Peralta, G. E. Scuseria, and R. L. Martin, J. Chem. Phys. **123**, 174101 (2005).
[31]G. Bergerhoff and I. D. Brown, *Crystallographic Databases* (International Union of Crystallography, Chester, 1987).
[32]H. L. Zhuang and R. G. Hennig, Appl. Phys. Lett. **103**, 212102 (2013).
[33]See supplementary material at http://dx.doi.org/10.1063/1.4891230 for the formation energies, structural parameters, phonon spectra, and band offsets of the 2D MX.
[34]H. L. Zhuang and R. G. Hennig, J. Phys. Chem. C **117**, 20440 (2013).
[35]A. Fleurence, R. Friedlein, T. Ozaki, H. Kawai, Y. Wang, and Y. Yamada-Takamura, Phys. Rev. Lett. **108**, 245501 (2012).
[36]S. Baroni, S. de Gironcoli, A. Dal Corso, and P. Giannozzi, Rev. Mod. Phys. **73**, 515 (2001).
[37]M. Gajdoš, K. Hummer, G. Kresse, J. Furthmüller, and F. Bechstedt, Phys. Rev. B **73**, 045112 (2006).
[38]P. Littlewood, J. Phys. C: Solid State Phys. **13**, 4855 (1980).
[39]R. N. Dexter, B. Lax, A. F. Kip, and G. Dresselhaus, Phys. Rev. **96**, 222 (1954).
[40]W. S. Yun, S. W. Han, S. C. Hong, I. G. Kim, and J. D. Lee, Phys. Rev. B **85**, 033305 (2012).
[41]J. Berashevich, O. Semeniuk, J. Rowlands, and A. Reznik, Europhys. Lett. **99**, 47005 (2012).
[42]H. L. Zhuang and R. G. Hennig, Phys. Rev. B **88**, 115314 (2013).